Infinitene: A Helically Twisted Figure-Eight [12]Circulene Topoisomer

Maciej Krzeszewski,[†] Hideto Ito,*,[†] and Kenichiro Itami*,[†,‡]

[†] Department of Chemistry, Graduate School of Science, Nagoya University, Nagoya 464-8602, Japan. [‡] Institute of Transformative Bio-Molecules (WPI-ITbM), Nagoya University, Nagoya 464-8602, Japan

This paper is dedicated to the memory of Prof. François Diederich.

ABSTRACT: New forms of molecular nanocarbons particularly looped polyarenes adopting various topologies contribute to the fundamental science and practical applications. Here we report on the synthesis of an infinity-shaped polycyclic aromatic hydrocarbon, infinitene **1** (cyclo[c.c.c.c.c.c.e.e.e.e.e.e]dodecakisbenzene) comprising consecutively fused 12-benzene rings forming an enclosed loop with a strain energy of 60.2 kcal·mol^{-1}. Infinitene **1** represents a topoisomer of still-hypothetical [12]circulene, and its scaffold can be formally visualized as the outcome of the "stitching" of two homochiral [6]helicene subunits by their both ends. The synthetic strategy encompasses transformation of a rationally designed dithiacyclophane to cyclophadiene through the Stevens rearrangement and pyrolysis of the corresponding S,S′-bis(oxide) followed by the UV-light mediated twofold photocyclization. The structure of infinitene **1** is a unique hybrid of helicene and circulene with a molecular formula $C_{48}H_{24}$, which can be regarded as an isomer for kekulene, [6,6]carbon nanobelt ([6,6]CNB), [12]cyclacene, and tetrabenzo[8]circulene as well. Infinitene **1** is a bench-stable yellow solid with green fluorescence, and soluble to common organic solvents. The figure-eight molecular structure of **1** was unambiguously confirmed by X-ray crystallography. The scaffold of **1**, reminiscent of a squeezed spring, stem from its enclosed, fully-fused architecture, is significantly compressed as manifested by a remarkably shortened distance (3.152–3.192 Å) between the centroids of two π-π stacked central benzene rings and the closest C···C distance of 2.920 Å. Combined lamellar and herringbone-like crystal packing suggested three-dimensional electronic interactions. Fundamental photophysical properties of infinitene **1** were thoroughly elucidated by means of UV-vis absorption and fluorescence spectroscopic studies as well as density functional theory (DFT) calculations. Its configurational stability enabled separation of the corresponding enantiomers (*P,P*) and (*M,M*) by a chiral HPLC. Circular dichroism (CD) and circularly polarized luminescence (CPL) measurements revealed that **1** has moderate $|g_{CD}|$ and $|g_{CPL}|$ values.
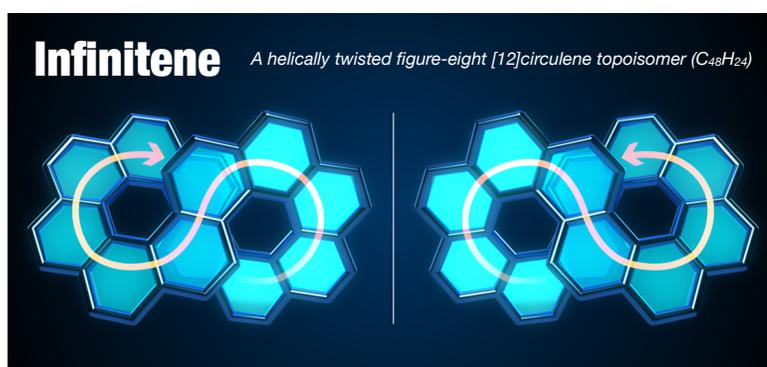
INTRODUCTION

Looped polyarenes adopting various topologies such as cycloarenes,[1-3] circulenes,[4] carbon nanobelts (CNB),[5,6] and cycloparaphenylenes[7] have drawn considerable attention in the scientific community. Not surprisingly, many of these synthetically challenging polycyclic aromatic hydrocarbons (PAHs) have been elusive for a long time. However, with the ongoing development of synthetic chemistry at large, many captivating scaffolds were obtained recently, enabling not only theoretical, but also practical investigations. These fascinating molecules contribute to the fundamental science, addressing long-standing questions regarding nature of aromaticity,[8] providing experimental evidences for the distribution of π-electrons in large polyaromatic systems.[9]

The prominent representatives of the cyclic polyarene family are kekulene[2] (cyclo[d.e.d.e.d.e.d.e.d.e]dodecakisbenzene[10], $C_{48}H_{24}$), and its structural isomers such as [6,6]CNB[5a] (cyclo[c.d.e.d.c.d.e.d.c.d.e.d]dodecakisbenzene[10]), and tetra-*cata*-tetrabenzo[8]circulene,[4d,e] as well as unexplored entities such as [12]cyclacene[6] (cyclo[d.d.d.d.d.d.d.d.d.d.d.d]dodecakisbenzene[10]) and [12]circulene[11] (cyclo[e.e.e.e.e.e.e.e.e.e.e.e]dodecakisbenzene[10]) (Figure 1a). Very interestingly, these "$C_{48}H_{24}$ family" include other structurally unique nanographenes[12] such as hexa-*peri*-hexabenzo[7]helicene[12a] (Figure 1a), hexa-*cata*-hexabenzocoronene,[12b] and benzo[1,2-*e*:3,4-*e′*:5,6-*e″*]triacephenanthrylene.[12c] These molecular nanocarbons can be considered as the structural motifs for the larger 2D and 3D systems such as graphene, helical graphene,[12a] fullerene/higher order bucky bowl,[12c,d] porous graphene sheet,[13] carbon nanotubes[14] and Mackay crystal.[15] These multidimensional carbon architectures were deemed to be potential game-changing materials displaying outstanding physical and mechanical properties. Undoubtedly, controlling size, shape and topology of the

nanocarbon structures is of utmost importance for fine tuning the features of final materials.[16]
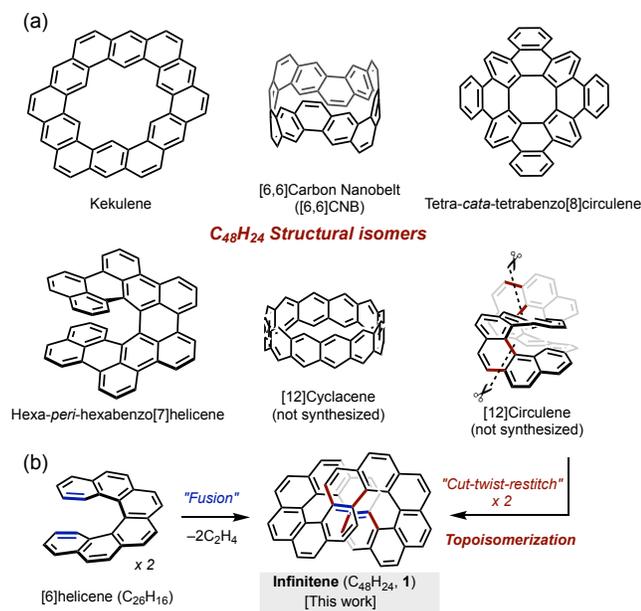
Figure 1. (a) Representative examples of structural isomers of $C_{48}H_{24}$. (b) Conceptual representation of an imaginary "fusion" and "cut-twist-restitch" leading to an infinity-shaped cycloarene "infinitene" (**1**).

Helicenes[17] represent yet another interesting class of *ortho*-fused polyaromatics which might be regarded as 'opened' analogs of circulenes. In recent years, chemistry of helicenes is undergoing a renaissance due to their exceptional properties, in particular, related to the intrinsic chirality and their application in materials science, supramolecular chemistry and asymmetric synthesis.[18] Our laboratory has long been involved in the creation of new forms of nanocarbon molecules. In particular, a range of twisted, nonplanar, molecular nanocarbons such as hybrid molecules of PAH and helicene, double-, triple, quadraple- and quintuple-helicenes, double-twisted aromatic macrocycles, axially chiral π-extended azulene, and all-benzene catenane and trefoil knot have been synthesized and studied in detail.[19]

As one of the ultimate targets with significant synthetic challenge, we have been interested in preparation of the entity, being a structural combination of circulene and helicene. Therefore, we designed an infinity-shaped cycloarene **1** (cyclo[*c.c.c.c.c.e.e.e.e.e.e*]dodecakisbenzene,[10] $C_{48}H_{24}$), merging traits of two aforementioned classes of polyaromatics. Formally, being a helically twisted analog of a saddle-shaped [12]circulene which is still a hypothetical molecule,[11] its structure can be viewed as the product of an imaginary fusion of both ends of two homochiral [6]helicenes in a head-to-head and tail-to-tail fashion (Figure 1b). Examples of helicenes which both ends are co-tethered such as helicenophanes[20] and cyclobishelicenes[21] are scarce, and at the inception of our work there were no reports on completely conjugated, helically twisted circulenes. During the preparation of this paper, Wu and Isobe recently reported the beautiful synthesis of a twisted, figure-eight CNB with persistent chirality.[22] Herein we present the successful synthesis of a fully fused, configurationally

unique, hybrid of helicene and circulene comprising twelve benzene rings ($C_{48}H_{24}$, **1**), dubbed *infinitene* due to its shape reminiscent of the infinity symbol.

RESULTS AND DISCUSSION

Design and Synthesis

Our molecular design of infinitene **1** was inspired by the historical synthesis of kekulene by Staab and Diederich that utilized a sequence of dithiacyclophane formation, sulfur extraction, cyclization, and endgame aromatization.[2b] As a bridge contraction through the Stevens rearrangement is well established and powerful strategy in the chemistry of cyclophanes,[20,23] we envisioned that sulfur-based, macrocyclization-annulation approach would lead to the first synthesis of infinity-shaped cycloarene **1** (Figure 2). In designing retrosynthesis of **1**, we became aware of the work of Matsubara and Yamamoto who have attempted to synthesize an analogous figure-eight cycloarene nearly twenty years ago.[24] Although they did not succeed in obtaining their target compound, they did report a successful synthesis of a strained macrocyclic dithioether through a double S_N2 reaction between 4,4′-bis(bromomethyl)-1,1′-biphenyl and dibenzo[*c,l*]chrysene-3,11-diyldimethanethiol. As the first step toward the first synthesis of **1**, we succeeded in the crucial macrocyclization of 3,9-bis(bromomethyl)chrysene (**2**) and dibenzo[*c,l*]chrysene-3,11-diyldimethanethiol (**3**) under the influence of Cs_2CO_3, furnishing dithiacyclophane macrocycle **4** in 25% yield (see SI for details). In this reaction, its rotamer **4′** and cyclic tetrasulfide **4″** (dimerization product of **3**) were also formed and isolated in 5% and 16% yield, respectively. Subsequently, we subjected **4** to the methylation reaction with dimethoxycarbenium tetrafluoroborate (the Borch reagent),[25] followed by NaH-mediated Stevens rearrangement of the thus-obtained salt. As a result, we obtained a complex mixture of stereoisomers of **5** in 57% yield. The resultant mixture was then subjected to the selective oxidation with 2.0 equivalents of *m*-CPBA to afford the corresponding *S,S*-bis(oxide) **6** in 99% yield as a mixture of isomers. Its pyrolysis at 500 °C under vacuum of 0.04–0.05 Torr gave cyclophadiene **7** in 46% yield. Finally, cyclophadiene **7** underwent smooth twofold photocyclization under UV-light giving the desired target molecule **1** in 89% yield as a bench-stable yellow solid (Figure 2). Unlike barely soluble kekulene, infinitene **1** shows good solubility toward common organic solvents such as $CHCl_3$, CH_2Cl_2, benzene and ethyl acetate, most likely due to its nonplanar structure.
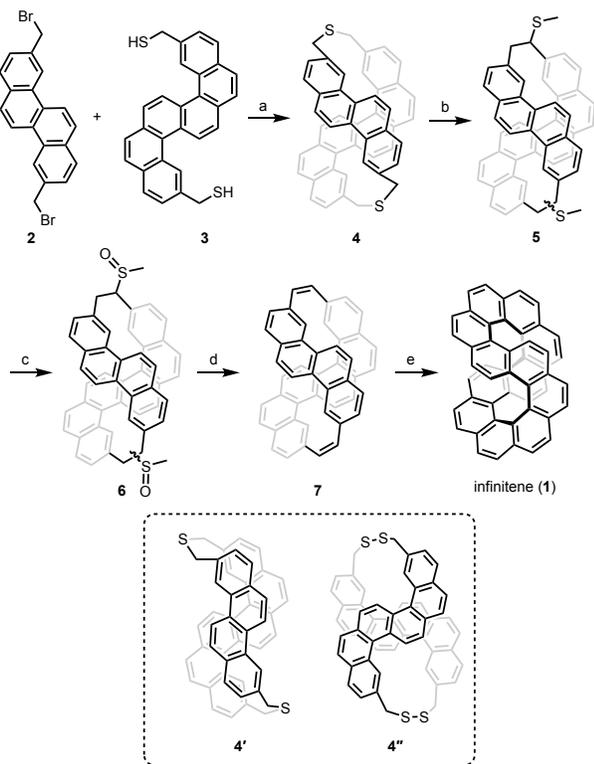
Figure 2. The synthetic pathway towards infinitene **1**. Reagents and conditions: (a) Cs_2CO_3 (1.1 equiv), DMF, 55 °C, 68 h, **4** (25%), **4'** (5%), **4"** (16%); (b) i) $(MeO)_2CHBF_4$ (6.0 equiv), CH_2Cl_2, 0 °C to r.t., 6 h, 95%, ii) NaH (10 equiv), THF, 55 °C, 48 h, 61% (overall 57% from **4** in two steps); (c) m-CPBA (2.0 equiv), CHCl$_3$, 0 °C to r.t., 13 h, 99%; (d) 500 °C, 0.04–0.05 Torr, 1 h, 46%; (e) I$_2$, *hv*, propylene oxide, C$_6$H$_6$, r.t., 6 h, 89%.

X-ray Crystallographic Analysis

The structure of infinitene **1** was unambiguously confirmed and analyzed by X-ray crystallography (Figure 3, Table S1 and Figures S2–S6). A suitable crystal was grown by recrystallization of a racemic mixture *rac*-**1** from a chloroform solution *via* slow vapor diffusion of methanol at room temperature. Infinitene **1** crystallized with the monoclinic space group $P2_1/n$ in the unit cell: a = 11.2861(11) Å, b = 13.3592(10) Å, c = 19.508(2) Å; α = 90°, β = 102.261(11)°, γ = 90°. The scaffold of **1**, reminiscent of a squeezed spring, stem from its enclosed, fully-fused architecture, is significantly compressed contrasting with unsubstituted helicenes. This is manifested by a remarkably shortened distance (3.152–3.192 Å) between the centroids of two π-π stacked central benzene rings and the closest C⋯C distance 2.920 Å (Figure 3a), compared to the analogous distance between the centroids of two terminal rings of unsubstituted [7]helicene, which reaches 3.804 Å (CCDC 852537).[26] The recent paper on similar figure-eight larger CNB by Wu also reported no interaction between intersected benzene rings.[22] Consequently, the splay angle of **1**, determined as the mean torsional angle of the corresponding inner [5]helicene subunit, was much shallower $\phi_{torsion}$= 20.34° than an analogous splay angle of [7]helicenes $\phi_{torsion}$= 24.35°. The end-to-end twist angle ϕ_{twist} of the junction naphthalene unit reached 22.03°.

The bond lengths of all convex-armchair edges (*K*-regions) vary only in the range of 1.334–1.359 Å suggesting their significant double bond character. The crystal packing structure indicates the strong three-dimensional intermolecular electronic interactions due to the fact that the (*P,P*)- and (*M,M*)-isomers of **1** tightly arranged themselves in a stacking array lacking any solvent molecules inside the crystal. Concurrently, the crystal packing reveals the presence of stacked lamellar homochiral molecular layers of each enantiomer lying on the *ab* plane interlacing each other along the *c*-axis (Figure 3c). The least-squares based mean planes of two intermolecular planes were separated by the length of 9.585 Å (Figure 3d) and the shortest contact between two heterochiral molecules was found between C(5) and H(16) atoms with a gap of 2.873 Å. At the same time, within the homochiral layer, tight herringbone arrangement along the *b*-axis can be observed (Figure 3e) with the closest intermolecular contact found between the C(1) and H(11) atoms of two different homochiral species with a separation of 2.819 Å (see SI for the packing and short contacts details).
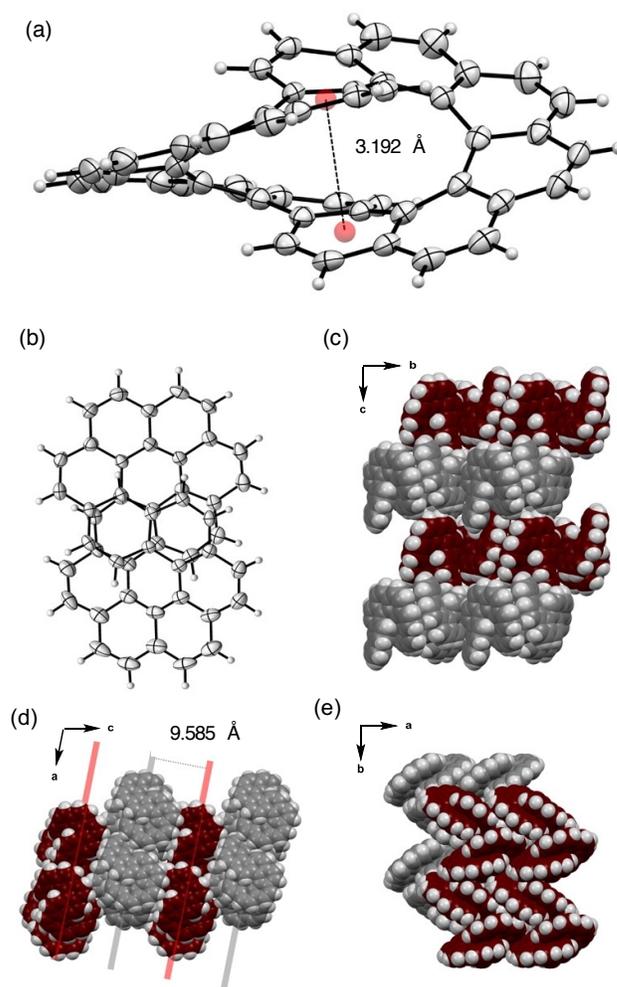
Figure 3. The X-ray crystal structure of **1**. (a) ORTEP drawing of the side view set at 50% probability level. (b) ORTEP drawing of the top view. (c-e) The crystal packing as a space-filling model, along *a*, *b* and *c* axes, respectively. (*P,P*)-**1** enantiomer colored in gray and (*M,M*)-**1** enantiomer colored in red.

UV-vis Absorption and Fluorescence Spectroscopy

UV-vis absorption and fluorescence spectra were measured in order to investigate the effect of the molecular configuration of 12 consecutively fused benzene rings of **1** on its electronic transitions (Figures 4 and S7–S9). The steady-state absorption and emission spectra revealed the basic optical properties of the final product possessing [8]helicene subunit in its structure. Infinitene **1** exhibits three main absorption bands with palpable, fine vibronic features. The first major band is located between 260 and 320 nm with a shoulder extending to 370 nm, showing two distinctive peaks at λ_{abs} = 294 and 311 nm with the molar extinction coefficients (ε) of 95,500 M^{-1} cm^{-1} and 59,000 M^{-1} cm^{-1}, respectively. The second band corresponding to the lower-energy transitions, found between 380 and 420 nm, also shows two peaks at λ_{abs} = 389 nm (ε = 14,800 M^{-1} cm^{-1}) and 412 nm (ε = 15,500 M^{-1} cm^{-1}). Finally, the third weak band, which corresponds to the longest wavelength absorption is located between 440 and 490 nm with the lowest-energy transition at λ_{abs}= 481 nm (ε = 1,350 M^{-1} cm^{-1}).

Infinitene **1** is a weak green light emitter with the maximum of emission located at λ_{em}= 505 nm (Figures 4 and S9). The Stokes shift was determined as 24 nm (988 cm^{-1}). Infinitene **1** displays bathochromic shift of the major absorption band (ca. 30 nm) with respect to both [8]helicene[27] and [12]helicene.[28] Emission curve of **1** is red-shifted by ca. 50 nm when compared to that of [8]helicene λ_{em}= 454 nm (22,050 cm^{-1})[29], and its emission maximum very closely matches with that of [12]helicene λ_{em}= 510 nm (19,600 cm^{-1}).[28] Finally, infinitene **1** exhibits slightly higher fluorescence quantum yield (Φ_F) of 0.038 than those of [8]helicene (0.014) and [12]helicene (0.0061).
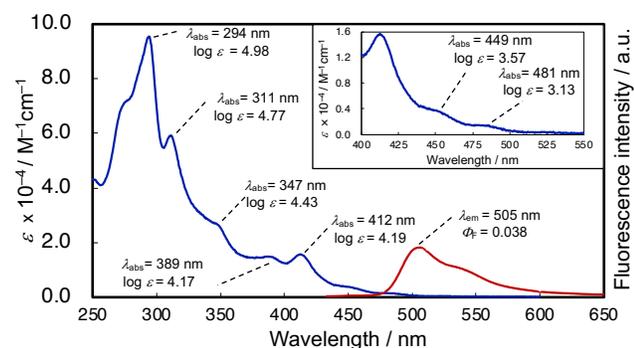
Figure 4. Absorption (blue line) and emission (red line) spectra of **1** measured in CH_2Cl_2. Absolute fluorescence quantum yield (Φ_F) determined with an integrating sphere.

Computational Study

To gain insight into the structure, π-conjugation, photophysical properties and strain energy of **1**, we performed computational studies by the density functional theory (DFT) method with a Gaussian 16 program.[30] Among various basis sets, the PBE0[31] functional well reproduced the structure obtained in X-ray crystallographic analysis (see Figure S14), and the structure optimization by PBE0/6-311+G(d,p) gave the most reasonable structure having a π-π stacking distance (3.192 Å) and the closest C···C distance (2.954 Å) (Figure 3a). Using this optimized structure, a NMR spectrum was calculated at the GIAO-DFT[32]/B3LYP[33]/6-311+G(2d,p) level of theory

in $CHCl_3$ with a SMD[34] solvent model. In the experimental ^1H-NMR spectrum of infinitene **1** (Figure 5a), there are six doublet peaks at σ (ppm) = 6.43, 6.99, 7.60, 8.04, 8.16, 8.18, whose values match well to the calculated chemical shifts (ppm) 6.48 (H_b), 7.04 (H_a), 7.65 (H_c), 8.05 (H_d), 8.22 (H_f) and 8.23 (H_e) (Figure 5b). It is reasonable that the only hydrogen atoms H_a and H_b were shielded due to an effect from ring current on a lower benzene ring. The calculated NICS[35](0) and NICS(1) values of representative three benzene rings are shown in Figure 5c, and a terminal benzene ring A indicated a slightly weakened aromatic nature compared to rings B and C. Considering the bond alternation found in the crystallographic structure and the computational studies, infinitene **1** has two equivalent Clar structures with six aromatic sextets and six double bonds (Figure 5d). Thus, all peripheral *K*-regions on infinitene **1** seem to have double bond nature like that on phenanthrene, implicating a potential of post-functionalization by annulative π-extension (APEX[36]) reactions or direct arylations[37] for further extended nanocarbon structures. Through a calculation of hypothetical homodesmotic reaction of **1** with benzene affording non-strained phenanthrene, the value of 60.2 kcal·mol^{-1} was estimated as a strain energy of **1** (Figure 5e).
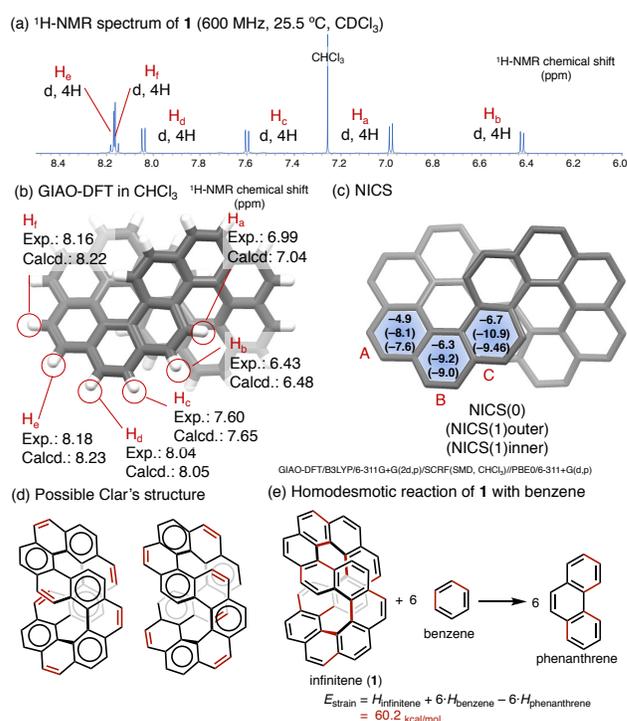
Figure 5. (a) Experimental ^1H NMR spectrum of infinitene **1** in the aromatic region (from 6.0 to 8.5 ppm) recorded in $CDCl_3$. (b) ^1H NMR chemical shift calculations. (c) NICS(0) values of **1**. NICS(1) values are shown in parentheses. (d) Possible Clar structures for **1**. (e) Determined strain energy of **1**.

We next performed time-dependent (TD)-DFT calculations at the B3LYP/6-311++G(d,p) level of theory for infinitene **1** geometry-optimized at the PBE0/6-311+G(d,p) level to elucidate six frontier molecular orbitals and absorptions (Figure 6). Each molecular orbital (MO) is found to be delocalized on entire molecule. While HOMO (−5.41 eV) and HOMO−1 (−5.76 eV) are delocalized only on benzene surface, the orbitals on intersectional center

naphthalene rings in LUMO (–2.21 eV) and LUMO+1 (–2.04 eV) are clearly overlapped. Existence of these through-space interactions is in good agreement with relatively low-lying energy levels of LUMO and LUMO+1. TD-DFT calculation revealed possible energy absorptions at a longer wavelength region: transitions from HOMO–1 to LUMO (2.57 eV, λ = 481 nm, oscillation strength (f) = 0.0001), HOMO to LUMO+1 (2.60 eV, λ = 477 nm, f = 0.0113), HOMO to LUMO+2 (2.76 eV, λ = 450 nm, f = 0.0024) and HOMO–1 to LUMO (2.89 eV, λ = 430 nm, f = 0.1226) were elucidated. The observed longest-wavelength absorption at 481 nm (Figure 4) can be assigned as forbidden HOMO–1 to LUMO and HOMO to LUMO+1 transitions, whereas weak absorption at 449 nm can be contributed by HOMO to LUMO+2 and HOMO–1 to LUMO transitions.
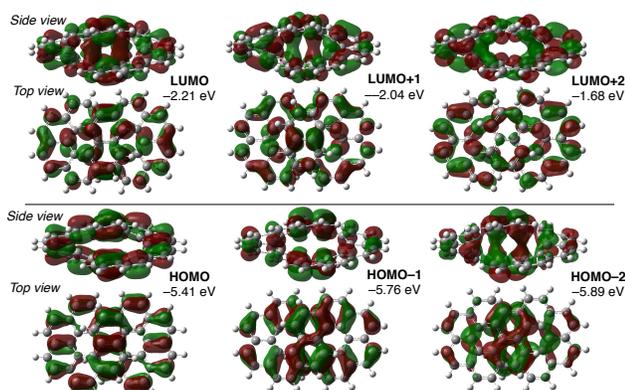
Figure 6. Pictorial representation of frontier molecular orbitals of infinitene **1**, and possible transitions calculated by TD-DFT. Isovalue = 0.02 was used for all depiction of MOs by GaussView 6.0.[38]

Chiral Separation and Chiroptical Properties

Intrinsic chirality of the helically twisted **1** prompted us to separate its respective enantiomers by a chiral HPLC. After extensive investigation, we found the optimal conditions for efficient separation of (P,P)-**1** and (M,M)-**1** enantiomers. The racemic mixture *rac*-**1** was successfully separated by a chiral HPLC (DAICEL CHIRALPAK® IE column; eluent: *n*-hexane/CH₂Cl₂ = 35:65) (Figure 7 inset and S10). The circular dichroism (CD) spectra of both enantiomers were recorded in CH₂Cl₂. The CD spectrum measured for the first fraction showed positive Cotton effect peaks at 239, 339 and 375 nm, whereas negative Cotton effect peaks were apparent in the range of 250–300 nm and at 415 nm (Figures 7, S11 and S12). The CD spectrum of the second fraction displayed perfect mirror symmetry, corroborating its opposite configuration. The intensities of the main bands of the molar circular dichroism ($\Delta\varepsilon$) with the local maxima located at 265, 339, 375 and 415 nm, as well as the anisotropy factors (g_{CD}) of the corresponding transitions were distinctively smaller than values reported for unsubstituted [n]helicenes, *e.g.* (P)-[6]helicene shows ($\Delta\varepsilon$) values of –267 M⁻¹ cm⁻¹ at 246 nm and +259 M⁻¹ cm⁻¹ at 324 nm.[39] The aforementioned molar circular dichroism values ($|\Delta\varepsilon|$) and anisotropy factors ($|g_{CD}|$) measured for **1** reached accordingly: 265 nm: $|\Delta\varepsilon|$ = 17.8 M⁻¹ cm⁻¹, $|g_{CD}|$ = $|\Delta\varepsilon/\varepsilon|$ = 3.5 × 10⁻⁴; 339 nm: $|\Delta\varepsilon|$ = 52.5 M⁻¹ cm⁻¹, $|g_{CD}|$ = 1.8 × 10⁻³ ; 375 nm: $|\Delta\varepsilon|$ = 69.0 M⁻¹ cm⁻¹, $|g_{CD}|$ = 4.8 × 10⁻³; 415 nm: $|\Delta\varepsilon|$ = 43.8 M⁻¹ cm⁻¹, $|g_{CD}|$

= 2.9 × 10⁻³; 457 nm: $|\Delta\varepsilon|$ = 10.4 M⁻¹ cm⁻¹, $|g_{CD}|$ = 3.4 × 10⁻³ and 484 nm: $|\Delta\varepsilon|$ = 3.0 M⁻¹ cm⁻¹, $|g_{CD}|$ = 2.3 × 10⁻³. The lower values of $|\Delta\varepsilon|$ and $|g_{CD}|$ are in agreement with the general trend set by the substitution effects on the chiroptical properties of helicenes, which are affected by a sophisticated interplay between geometric and electronic factors.[40]

Concurrently, unlike large values of optical rotation reported for pristine [n]helicenes, for example (P)-[6]helicene: $[a]^{25}_D$ = +3707° (CHCl₃)[41] and (P)-[7]helicene: $[a]^{25}_D$ = +5577° (CHCl₃),[42] infinitene **1** shows significantly smaller values of $[a]^{20}_D$ = +1130° (c = 8.9 × 10⁻³ M in CH₂Cl₂) in the case of the first fraction (99.98% ee) and $[\alpha]^{20}_D$ = –1112° (c = 8.6 × 10⁻³ M in CH₂Cl₂) for the second fraction (99.90% ee). As a rule of thumb in the chemistry of carbohelicenes, levorotary (–) enantiomers tend to adopt left-handed (M) configuration, whereas dextrorotary (+) compounds are mainly, right-handed (P).[17c,39] In addition, TD-DFT calculation of both enantiomers also supported that the first fraction (blue line) and the second fraction (red line) were expected to be to be (P,P)-**1** and (M,M)-**1**, respectively (Figure S15).
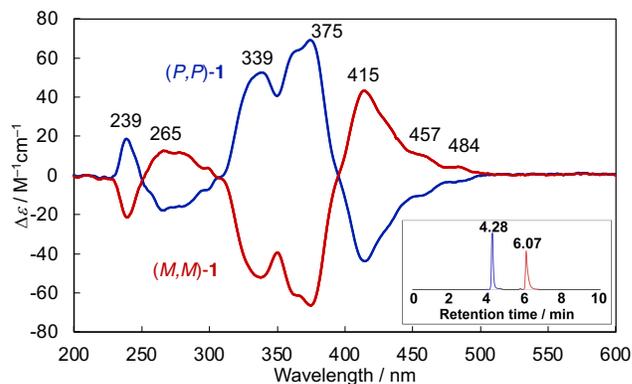
Figure 7. Circular dichroism spectra of the enantiomers of **1** measured in CH₂Cl₂. An inset shows a chromatograph obtained in chiral HPLC analysis of the racemic mixture of **1**, eluted with *n*-hexane/CH₂Cl₂ (35:65) using DAICEL CHIRALPAK® IE column (horizontal axis: retention time; vertical axis: detector absorption intensity at 315 nm). Spectra were shown as blue lines (the first eluted fraction) and red lines (the second eluted fraction).

Recently, circularly polarized luminescence (CPL) of helicene derivatives were reported with rational designs for higher dissymmetry factor (g_{CPL}),[43] and some of related figure-eight-shaped molecules show 10⁻² to 10⁻³ order values of g_{CPL}, whose values are relatively higher than simple carbohelicenes.[44] Stimulated by these examples, CPL of both enantiomers of **1** was also measured (Figures 8 and S13). (P,P)-**1** and (M,M)-**1** displayed –6.2 × 10⁻³ and 6.4 × 10⁻³ of g_{CPL}, which are reasonable values when considering the same order value of $|g_{CD}|$. Although infinitene **1** did not show extremely high values of $|g_{CPL}|$ and the structure-CPL ability relationship is still unclear, we believe that our new example of shape-persistent, symmetric and fully-conjugated, infinity-shaped molecule will help further molecular design to increase the g_{CPL} value.
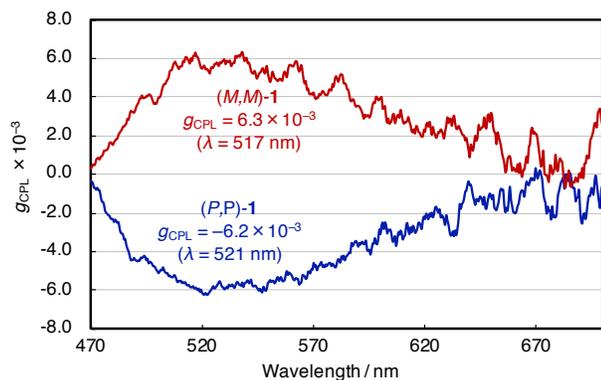
Figure 8. Circularly polarized luminescence (CPL) spectra of (*P,P*)-**1** (blue line) and (*M,M*)-**1** (red line) recorded on a JASCO CPL-300 spectrofluoropolarimeter at 25 °C with a 10 × 10 mm cells under the following conditions: scattering angle: 0°, excitation slit width: 5 nm, emission slit width: 5 nm, scan rate: 100 nm min⁻¹, response: 4 sec, accumulation: 8 times; data interval: 0.5 nm, solvent: CH_2Cl_2, sample concentrations: 2.4×10^{-6} M for (*P,P*)-**1** and 2.9×10^{-6} M for (*M,M*)-**1**, excitation wavelength: 370 nm, HT voltage (photomultiplier): 650 V.

CONCLUSIONS

In summary, we have accomplished the synthesis of infinitene **1** (cyclo[*c.c.c.c.c.e.e.e.e.e.e*]dodecakisbenzene), a unique, fully fused, helically twisted [12]circulene topoisomer. We have studied its fundamental properties experimentally as well as computationally. The intrinsic chirality of **1** enabled successful separation of the enantiomers by a chiral HPLC resulting in an investigation of their chiroptical properties. The infinity-shaped geometry of **1** was unequivocally confirmed by X-ray diffraction analysis. Its crystal structure revealed significant compression of the central [8]helicene subunit, manifested by a close distance of 3.152–3.192 Å between two π-π stacked benzene rings. Combined lamellar and herringbone-like crystal packing suggested three-dimensional electronic interactions. CD and CPL measurements revealed that **1** has moderate |g_{CD}| and |g_{CPL}| values as same as other figure-eight-shaped molecules. These results open the new chapter in the chemistry of fully-fused, looped polyarenes. The established successful synthetic strategy would be an incentive to envision and create new amazing forms of nanocarbons whose architectures are limited only by our imagination.

ASSOCIATED CONTENT

Supporting Information
Experimental procedures, ¹H and ¹³C NMR spectra, characterization of data for all new compounds, optical properties, computational data and crystallographic data of **1**.

Accession codes
CCDC 2113525 contains the supplementary crystallographic data for this paper. These data can be obtained free of charge via www.ccdc.cam.ac.uk/data_request/cif, or by emailing data_request@ccdc.cam.ac.uk, or by contacting The Cambridge Crystallographic Data Centre, 12 Union Road, Cambridge CB2 1EZ, UK; fax: +44 1223 336033.

AUTHOR INFORMATION

Corresponding Author
* itami@chem.nagoya-u.ac.jp (K.I.)
* ito.hideto@g.mbox.nagoya-u.ac.jp (H.I.)

Author Contributions
M.K. designed, synthesized and characterized all compounds. H.I. supervised the experiments and performed the theoretical calculations. K.I. directed the whole project. The manuscript was written through contributions of all authors. All authors have given approval to the final version of the manuscript.

REFERENCES

(1) For an excellent review, see: Buttrick, J. C.; King, B. T. Kekulenes, cycloarenes, and heterocycloarenes: addressing electronic structure and aromaticity through experiments and calculations. *Chem. Soc. Rev.* **2017**, *46*, 7-20.

(2) Kekulene: (a) Krieger, C.; Diederich, F.; Schweitzer, D.; Staab, H. A. Molecular Structure and Spectroscopic Properties of Kekulene. *Angew. Chem., Int. Ed. Engl.* **1979**, *18*, 699-701. (b) Staab, H. A.; Diederich, F. Synthesis of Kekulene. *Chem. Ber.* **1983**, *116*, 3487-3503. (c) Staab, H. A.; Diederich, F.; Krieger, C.; Schweitzer, D. Molecular Structure and Spectroscopic Properties of Kekulene. *Chem. Ber.* **1983**, *116*, 3504-3512. (d) Vögtle, F.; Staab, H. A. Versuche zur Darstellung des Cyclo[*d.e.d.e.d.e.d.e.d.e.d.e*]dodecakisbenzens. Eine neue Synthese von 1.2;7.8-Dibenzo-anthracenen. *Chem. Ber.* **1968**, *101*, 2709-2716. (e) Pozo, I.; Majzik, Z.; Pavliček, N.; Melle-Franco, M.; Guitián, E.; Peña, D.; Gross, L.; Pérez, D. Revisiting Kekulene: Synthesis and Single-Molecule Imaging. *J. Am. Chem. Soc.* **2019**, *141*, 15488-15493.

(3) Other representative cycloarenes: (a) Funhoff, D. J. H. & Staab, H. A. Cyclo[*d.e.d.e.e.d.e.d.e.e*]decakisbenzene, a new cycloarene. *Angew. Chem., Int. Ed. Engl.* **1986**, *25*, 742-744. (b) Kumar, B.; Viboh, R. L.; Bonifacio, M. C.; Thompson, W. B.; Buttrick, J. C.; Westlake, B. C.; Kim, M.-S.; Zoellner, R. W.; Varganov, S. A.; Mörschel, P.; Teteruk, J.; Schmidt, M. U.; King, B. T. Septulene: The Heptagonal Homologue of Kekulene. *Angew. Chem., Int. Ed.* **2012**, *51*, 12795-12800. (c) Majewski, M. A.; Lis, T.; Cybińska, J.; Stępień. M. Chrysaorenes: assembling coronoid hydrocarbons *via* the fold-in synthesis. *Chem. Commun.* **2015**, *51*, 15094-15097. (d) Majewski, M. A.; Hong, Y.; Lis, T.; Gregoliński, J.; Chmielewski, P. J.; Cybińska, J.; Kim, D.; Stępień, M. Octulene: A Hyperbolic Molecular Belt that Binds Chloride Anions. *Angew. Chem., Int. Ed.* **2016**, *55*, 14072-14076. (e) Hou, H.; Zhao, X.-J.; Tang, C.; Ju, Y.-Y.; Deng, Z.-Y.; Wang, X.-R.; Feng, L.-B.; Lin, D.-H.; Hou, X.; Narita, A.; Müllen, K.; Tan, Y.-Z. Synthesis and assembly of extended quintulene. *Nat. Commun.* **2020**, *11*, 3976. (f) Fan, W.;

Han, Y.; Wang, X.; Hou, X.; Wu, J. Expanded Kekulenes. *J. Am. Chem. Soc.* **2021**, *143*, 13908-13916.

(4) Some representative circulenes: (a) Yamamoto, K.; Harada, T.; Nakazaki, M.; Naka, T.; Kai, Y.; Harada, S.; Kasai, N. Synthesis and Characterization of [7]Circulene. *J. Am. Chem. Soc.* **1983**, *105*, 7171-7172. (b) Bharat, Bhola, R.; Bally, T.; Valente, A.; Cyrański, M. K.; Dobrzycki, Ł.; Spain, S. M.; Rempała, P.; Chin, M. R.; King, B. T. Quadrannulene: A Nonclassical Fullerene Fragment. *Angew. Chem., Int. Ed.* **2010**, *49*, 399-402. (c) Feng, C.-N.; Kuo, M.-Y.; Wu, Y.-T. Synthesis, Structural Analysis, and Properties of [8]Circulenes. *Angew. Chem., Int. Ed.* **2013**, *52*, 7791-7794. (d) Sakamoto, Y.; Suzuki, T. Tetrabenzo[8]circulene: Aromatic Saddles from Negatively Curved Graphene. *J. Am. Chem. Soc.* **2013**, *135*, 14074-14077. (e) Miller, R. W.; Duncan, A. K.; Schneebeli, S. T.; Gray, D. L.; Whalley, A. C. Synthesis and Structural Data of Tetrabenzo[8]circulene. *Chem. Eur. J.* **2014**, *20*, 3705-3711.

(5) Carbon nanobelts: (a) Povie, G.; Segawa, Y.; Nishihara, T.; Miyauchi, Y.; Itami, K. Synthesis of a carbon nanobelt. *Science* **2017**, *356*, 172-175. (b) Povie, G.; Segawa, Y.; Nishihara, T.; Miyauchi, Y.; Itami, K. Synthesis and Size-Dependent Properties of [12], [16], and [24]Carbon Nanobelts. *J. Am. Chem. Soc.* **2018**, *140*, 10054-10059. (c) Cheung, K. Y.; Gui, S.; Deng, C.; Liang, H.; Xia, Z.; Liu, Z.; Chi, L.; Miao, Q. Synthesis of Armchair and Chiral Carbon Nanobelts. *Chem* **2019**, *5*, 838-847. (d) Cheung, K. Y.; Watanabe, K.; Segawa, Y.; Itami, K. Synthesis of a zigzag carbon nanobelt. *Nat. Chem.* **2021**, *13*, 255-259. (e) Han, Y.; Dong, S.; Shao, J.; Fan, W.; Chi, C. Synthesis of a Sidewall Fragment of a (12,0) Carbon Nanotubes. *Angew. Chem., Int. Ed.* **2021**, *60*, 2658-2662. (f) Xia, Z.; Pun, S. H.; Chen, H.; Miao, Q. Synthesis of Zigzag Carbon Nanobelts through Scholl Reactions. *Angew. Chem., Int. Ed.* **2021**, *60*, 10311-10318.

(6) For an excellent recent review on aromatic hydrocarbon belts including cyclacenes, see: (a) Guo, Q.-H.; Qiu, Y.; Wang, M.-X.; Stoddart, J. F. Aromatic hydrocarbon belts. *Nat. Chem.* **2021**, *13*, 402-419. For early works, see: (b) Heilbronner, E. Molecular Orbitals in homologen Reihen mehrkerniger aromatischer Kohlenwasserstoffe: I. Die Eigenwerte yon LCAO-MO's in homologen Reihen. *Helv. Chim. Acta* **1954**, *37*, 921-935. (c) Vögtle, F. Concluding Remarks. *Top. Curr. Chem.* **1983**, *115*, 157-159. (d) Kohnke, F. H.; Slawin, A. M. Z.; Stoddart, J. F.; Williams, D. J. Molecular Belts and Collars in the Making: A Hexaepoxyoctacosahydro[12]cyclacene Derivative. *Angew. Chem., Int. Ed. Engl.* **1987**, *26*, 892-894. (e) Ashton, P. R.; Isaacs, N. S.; Kohnke, F. H.; Slawin, A. M. Z.; Spencer, C. M.; Stoddart, J. F.; Williams, D. J. Towards the Making of [12]Collarene. *Angew. Chem., Int. Ed. Engl.* **1988**, *27*, 966-969.

(7) (a) Jasti, R.; Bhattacharjee, J.; Neaton, J. B.; Bertozzi, C. R. Synthesis, Characterization, and Theory of [9]-, [12]-, and [18]Cycloparaphenylene: Carbon Nanohoop Structures. *J. Am. Chem. Soc.* **2008**, *130*, 17646-17647. (b) Takaba, H.; Omachi, H.; Yamamoto, Y.; Bouffard, J.; Itami, K. Selective Synthesis of [12]Cycloparaphenylene. *Angew. Chem., Int. Ed.* **2009**, *48*, 6112- 6116. (c) Yamago, S.; Watanabe, Y.; Iwamoto, T. Synthesis of [8]Cycloparaphenylene from a Square-Shaped Tetranuclear Platinum Complex. *Angew. Chem., Int. Ed.* **2010**, *49*, 757-759. For selected reviews, see: (d) Tian, X.; Jasti, R. Cycloparaphenylenes: The Shortest Possible Segments of Armchair Carbon Nanotubes. *In Fragments of Fullerenes and Carbon Nanotubes* **2011**, 291-309. (e) Segawa, Y.; Yagi, A.; Matsui, K.; Itami, K. Design and Synthesis of Carbon Nanotube Segments. *Angew. Chem., Int. Ed.* **2016**, *55*, 5136-5158. (f) Leonhardt, E. J.; Jasti, R. Emerging applications of carbon nanohoops. *Nat. Rev. Chem.* **2019**, *3*, 672-686. (g) Li, Y.; Kono, H.; Maekawa, T.; Segawa, Y.; Yagi, A.; Itami, K. Chemical Synthesis of Carbon Nanorings and Nanobelts. *Acc. Mater. Res.* **2021**, *2*, 681-691.

(8) (a) Aihara, J. π-Electron Currents Induced in Polycyclic Benzenoid Hydrocarbons and Their Relationship to Clar Structures. *J. Phys. Chem. A* **2003**, *107*, 11553-11557. (b) Randic, M. Aromaticity of Polycyclic Conjugated Hydrocarbons. *Chem. Rev.* **2003**, *103*, 3449-3605. (c) Aihara, J.; Makino, M. Constrained Clar Formulas of Coronoid Hydrocarbons. *J. Phys. Chem. A* **2014**, *118*, 1258-1266. (d) Liu, C.; Ni, Y.; Lu, X.; Li, G.; Wu, J. Global Aromaticity in Macrocyclic Polyradicaloids: Hückel's Rule or Baird's Rule? *Acc. Chem. Res.* **2019**, *52*, 2309-2321.

(9) (a) Lu, X.; Lee, S.; Hong, Y.; Phan, H.; Gopalakrishna, T. Y.; Herng, T. S.; Tanaka, T.; Sandoval-Salinas, M. E.; Zeng, W.; Ding, J.; Casanova, D.; Osuka, A.; Kim, D.; Wu, J. Fluorenyl Based Macrocyclic Polyradicaloids. *J. Am. Chem. Soc.* **2017**, *139*, 13173-13183. (b) Lu, X.; Gopalakrishna, T. Y.; Phan, H.; Herng, S. T.; Jiang, Q.; Liu, C.; Li, G.; Ding, J.; Wu, J. Global Aromaticity in Macrocyclic Cyclopenta-Fused Tetraphenanthrenylene Tetraradicaloid and Its Charged Species. *Angew. Chem., Int. Ed.* **2018**, *57*, 13052-13056. (c) Liu, C.; Sandoval-Salinas, M. A.; Hong, Y.; Gopalakrishna, T. Y.; Phan, H.; Aratani, N.; Herng, T. S.; Ding, J.; Yamada, H.; Kim, D.; Casanova, D.; Wu. J. Macrocyclic Polyradicaloids with Unusual Super-ring Structure and Global Aromaticity. *Chem* **2018**, *4*, 1586-1595.

(10) In this paper, we use the Staab-Vögtle-Diederich nomenclature for cycloarenes. See ref 1, 2b, and 2d for the definition.

(11) Christoph, H.; Grunenberg, J.; Hopf, H.; Dix, I.; Jones, P. G.; Scholtissek, M.; Maier, G. MP2 and DFT Calculations on Circulenes and an Attempt to Prepare the Second Lowest Benzelog, [4]Circulene. *Chem. Eur. J.* **2008**, *14*, 5604-5616.

(12) (a) Nakakuki, Y.; Hirose, T.; Sotome, H.; Miyasaka, H.; Matsuda, K. Hexa-*peri*-hexabenzo[7]helicene: Homogeneously π-Extended Helicene as a Primary Substructure of Helically Twisted Chiral Graphenes. *J. Am. Chem. Soc.* **2018**, *140*, 4317-4326. (b) Clar, E.; Stephen, J. F. The synthesis of 1:2, 3:4, 5:6, 7:8, 9:10, 11:12-hexabenzocoronene. *Tetrahedron* **1965**, *21*, 467-470. (c) de Frutos, Ó.; Gomez-Lor, B.; Granier, T.; Monge, M.Á.; Gutiérrez-Puebla, E.; Echavarren, A. M. Syn-Trialkylated Truxenes: Building Blocks That Self-Associate by Arene Stacking. *Angew. Chem., Int. Ed.* **1999**, *38*, 204-207. (d) Mehta, G.; Sarma, P. P. V. S. A rapid, two step construction of novel $C_{48}H_{24}$ and $C_{54}H_{24}$ polycyclic aromatic hydrocarbons represented on the C_{60}-fullerene surface via a threefold intramolecular Heck coupling reaction. *Tetrahedron Lett.* **2002**, *43*, 6557-6560. (e) Liu, P.; Chen, X.-Y.; Cao, J.; Ruppenthal, L.; Gottfried, J. M.; Müllen, K.; Wang, X.-Y. Revisiting Acepleiadylene: Two-Step Synthesis and π-Extension toward Nonbenzenoid Nanographene. *J. Am. Chem. Soc.* **2021**, *143*, 5314-5318. (f) Sumy, D. P.; Finkeb, A. D.; Whalley, A. C. The reductive aromatization of tridecacyclene. *Chem. Commun.* **2016**, *52*, 12368-12371.

(13) (a) Robertson, A. W.; Lee, G.-D.; He, K.; Gong, C.; Chen, Q.; Yoon, E.; Kirkland, A. I.; Warner, J. H. Atomic Structure of Graphene Subnanometer Pores. *ACS Nano* **2015**, *9*, 11599-11607. (b) Beser, U.; Kastler, M.; Maghsoumi, A.; Wagner, M.; Castiglioni, C.; Tommasini, M.; Narita, A.; Feng, X.; Müllen, K. A C216-Nanographene Molecule with Defined Cavity as Extended Coronoid. *J. Am. Chem. Soc.* **2016**, *138*, 4322-4325. (c) Moreno, C.; Vilas-Varela, M.; Kretz, B.; García-Lekue, A.; Costache, M. V.; Paradinas, M.; Panighel, M.; Ceballos, G.; Valenzuela, S. O.; Peña, D.; Mugarza, A. Bottom-up synthesis of multifunctional nanoporous graphene. *Science* **2018**, *360*, 199-203. (d) Xu, K.; Urgel, J. I.; Eimre, K.; Di Giovannantonio, M.; Keerthi, A.; Komber, H.; Wang, S.; Narita, A.; Berger, R.; Ruffieux, P.; Pignedoli, C. A.; Liu, J.; Müllen, K.; Fasel, R.; Feng, X. On-Surface Synthesis of a Nonplanar Porous Nanographene. *J. Am. Chem. Soc.* **2019**, *141*, 7726-7730.

(14) (a) Iijima, S. Helical microtubules of graphitic carbon. *Nature* **1991**, *354*, 56-58. (b) Dresselhaus, M.; Dresselhaus, G.; Avouris, P. *Carbon Nanotubes: Synthesis Properties, Applications*; Springer: Berlin, 2001. (c) Liu, B.; Wu, F.; Gui, H.; Zheng, M.; Zhou, C. Chirality-Controlled Synthesis and Applications of Single-Wall Carbon Nanotubes. *ACS Nano* **2017**, *11*, 31-53.

(15) (a) Mackay, A. L.; Terrones, H. Diamond from graphite. *Nature* **1991**, *352*, 762. (b) Tagamia, M.; Liang, Y.; Naito, H.; Kawazoe, Y.; Kotani, M. Negatively curved cubic carbon crystals with octahedral symmetry. *Carbon* **2014**, *76*, 266-274. (c) Matsubara, S.; Koga, Y.; Segawa, Y.; Murakami, K.; Itami, K. Creation of negatively curved polyaromatics enabled by annulative coupling that forms an eight-membered ring. *Nat. Catal.* **2020**, *3*, 710-718.

(16) (a) Segawa, Y.; Ito, H.; Itami, K. Structurally uniform and atomically precise carbon nanostructures. *Nat. Rev. Mater.* **2016**, *1*, 15002. (b) Segawa, Y.; Levine, D. R.; Itami, K. Topologically Unique Molecular Nanocarbons. *Acc. Chem. Res.* **2019**, *52*, 2760-2767.

(17) (a) Shen, Y.; Chen, C.-F. Helicenes: Synthesis and Applications. *Chem. Rev.* **2012**, *112*, 1463-1535. (b) Gingras, M. One hundred years of helicene chemistry. Part 1: non-stereoselective syntheses of carbohelicenes. *Chem. Soc. Rev.* **2013**, *42*, 968-1006. (c) Gingras, M.; Félix, G.; Peresuttiab, R. One hundred years of helicene chemistry. Part 2: stereoselective syntheses and chiral separations of carbohelicenes. *Chem. Soc. Rev.* **2013**, *42*, 1007-1050. (d) Gingras, M. One hundred years of helicene chemistry. Part 3: applications and properties of carbohelicenes. *Chem. Soc. Rev.* **2013**, *42*, 1051-1095. (e) Rickhaus, M.; Mayor, M.; Juríček, M. Strain-induced helical chirality in polyaromatic systems. *Chem. Soc. Rev.* **2016**, *45*, 1542-1556. (f) Kato, K.; Segawa, Y.; Itami, K. Symmetric Multiple Carbohelicenes. *Synlett* **2019**, *30*, 370-377.

(18) (a) Jančařík, A.; Rybáček, A.; Cocq, K.; Chocholoušová, J. V.; Vacek, J.; Pohl, R.; Bednárová, L.; Fiedler, P.; Císařová, I.; Stará, I. G.; Starý, I. Rapid Access to Dibenzohelicenes and their Functionalized Derivatives. *Angew. Chem., Int. Ed.* **2013**, *52*, 9970-9975. (b) Krzeszewski, M.; Kodama, T.; Espinoza, E. M.; Vullev, V. I.; Kubo, T.; Gryko, D. T. Nonplanar Butterfly-Shaped π-Expanded Pyrrolopyrroles. *Chem. Eur. J.* **2016**, *22*, 16478-16488. (c) Hosokawa, T.; Takahashi, Y.; Matsushima, T.; Watanabe, S.; Kikkawa, S.; Azumaya, I.; Tsurusaki, A.; Kamikawa, K. Synthesis, Structures, and Properties of Hexapole Helicenes: Assembling Six [5]Helicene Substructures into Highly Twisted Aromatic Systems. *J. Am. Chem. Soc.* **2017**, *139*, 18512-18521. (d) Malik, A. U.; Gan, F.; Shen, C.; Yu, N.; Wang, R.; Crassous, J.; Shu, M.; Qiu, H. Chiral Organic Cages with a Triple-Stranded Helical Structure Derived from Helicene. *J. Am. Chem. Soc.* **2018**, *140*, 2769-2772. (e) Nakakuki, Y.; Hirose, T.; Matsuda, K. Synthesis of a Helical Analogue of Kekulene: A Flexible π-Expanded Helicene with Large Helical Diameter Acting as a Soft Molecular Spring. *J. Am. Chem. Soc.* **2018**, *140*, 15461-15469. (f) Reger, D.; Haines, P. Heinemann, F.; W. Guldi, D. M.; Jux, N. Oxa[7]superhelicene: A π-Extended Helical Chromophore Based on Hexa-*peri*-hexabenzocoronenes. *Angew. Chem., Int. Ed.* **2018**, *57*, 5938-5942. (g) Evans, P. J.; Ouyang, J.; Favereau, L.; Crassous, J.; Fernández, I.; Perles, J.; Martín, N. Synthesis of a Helical Bilayer Nanographene. *Angew. Chem., Int. Ed.* **2018**, *57*, 6774-6779. (h) Liu, G.; Koch, T.; Li, Y.; Doltsinis, N. L.; Wang, Z. Nanographene Imides Featuring Dual-Core Sixfold [5]Helicenes. *Angew. Chem., Int. Ed.* **2019**, *58*, 178-183. (i) Yubuta, A.; Hosokawa, T.; Gon, M.; Tanaka, K.; Chujo, Y.; Tsurusaki, A.; Kamikawa, K. Enantioselective Synthesis of Triple Helicenes by Cross-Cyclotrimerization of a Helicenyl Aryne and Alkynes via Dynamic Kinetic Resolution. *J. Am. Chem. Soc.* **2020**, *141*, 10025-100033.

(19) (a) Fujikawa, T.; Segawa, Y.; Itami, K. Synthesis, Structures, and Properties of π-Extended Double Helicene: A Combination of Planar and Nonplanar π-Systems. *J. Am. Chem. Soc.* **2015**, *137*, 7763-7768. (b) Fujikawa, T.; Segawa, Y.; Itami, K. Synthesis and Structural Features of Quadruple Helicenes: Highly Distorted π Systems Enabled by Accumulation of Helical Repulsions. *J. Am. Chem. Soc.* **2016**, *138*, 3587-3595. (c) Fujikawa, T.; Preda, D. V.; Segawa, Y.; Itami, K.; Scott, L. T. Corannulene-Helicene Hybrids: Chiral π-Systems Comprising Both Bowl and Helical Motifs. *Org. Lett.* **2016**, *18*, 3992-3995. (d) Kato, K.; Segawa, Y.; Itami, K. Phenanthro[9,10-a]corannulene by one-step annulative π-extension of corannulene. *Can. J. Chem.* **2017**, *95*, 329-333. (e) Fujikawa, T.; Mitoma, N.; Wakamiya, A.; Saeki, A.; Segawa, Y.; Itami, K. Synthesis, Properties, and Crystal Structures of π-Extended Double [6]Helicenes: Contorted Multi-Dimensional Stacking Lattices. *Org. Biomol. Chem.* **2017**, *15*, 4697-4703. (f) Fujikawa, T.; Segawa, Y.; Itami, K. Laterally π-Extended Dithia[6]helicenes with Heptagons: Saddle-Helix Hybrid Molecules. *J. Org. Chem.* **2017**, *82*, 7745-7749. (g) Kato, K.; Segawa, Y.; Scott, L. T.; Itami, K. A Quintuple [6]Helicene with a Corannulene Core as a C_5-symmetric Propeller-shaped π-System. *Angew. Chem., Int. Ed.* **2018**, *57*, 1337-1341. (h) Kawai, K.; Kato, K.; Peng, L.; Segawa, Y.; Scott, L. T.; Itami, K. Synthesis and Structure of a Propeller-Shaped Polycyclic Aromatic

Hydrocarbon Containing Seven-Membered Rings. *Org. Lett.* **2018**, *20*, 1932-1935. (i) Lin, H.-A.; Kato, K.; Segawa, Y.; Scott, L. T.; Itami, K. Synthesis and Structural Features of Thiophene-fused Analogues of Warped Nanographene and Quintuple Helicene. *Chem. Sci.* **2019**, *10*, 2326-2330. (j) Chaolumen, Ito, H.; Itami, K. An Axially Chiral 1,1′-Biazulene and its π-Extended Derivative: Synthesis, Structures and Properties. *Chem. Commun.* **2019**, *55*, 9606-9609. (k) Segawa, Y.; Kuwayama, M.; Hijikata, Y.; Fushimi, M.; Nishihara, T.; Pirillo, J.; Shirasaki, J.; Kubota, N.; Itami K. Topological molecular nanocarbons: All-benzene catenane and trefoil knot. *Science* **2019**, *365*, 272-276. (l) Li, Y.; Yagi, A.; Itami, K. Synthesis of Highly Twisted, Nonplanar Aromatic Macrocycles Enabled by Axially Chiral 4,5-Diphenylphenanthrene Building Block. *J. Am. Chem. Soc.* **2020**, *142*, 3246-3253. (m) Watanabe, K.; Segawa, Y.; Itami, K. A Theoretical Study on the Strain Energy of Helicene-Containing Carbon Nanobelts. *Chem. Commun.* **2020**, *56*, 15044-15047.

(20) Ghasemabadi, P. G.; Yao, T, Bodwell, G. J. Cyclophanes containing large polycyclic aromatic hydrocarbons. *Chem. Soc. Rev.* **2015**, *44*, 6494-6518.

(21) (a) Thulin, B.; Wennerström, O. Propellicene or Bi-2,13-pentahelicenylene. *Acta Chem. Scand.* **1976**, *B 30*, 688-690. (b) Thulin, B.; Wennerström, O. Synthesis of [2.0.2.0]metacyclophanediene and bi-4,5-phenanthrylene. *Tetrahedron Lett.* **1977**, *18*, 929-930. (c) Matsuno, T.; Kogashi, K.; Sato, S.; Isobe, H. Enhanced yet Inverted Effects of π-Extension in Self-Assembly of Curved π-Systems with Helicity. *Org. Lett.* **2017**, *19*, 6456-6459. (d) Robert, A.; Dechambenoit, P.; Hillard, E. A.; Bock, H.; Durola, F. Non-planar oligoarylene macrocycles from biphenyl. *Chem. Commun.* **2017**, *53*, 11540-11543. (e) Robert, A.; Naulet, G.; Bock, H.; Vanthuyne, N.; Jean, M.; Giorgi, M.; Carissan, Y.; Aroulanda, C.; Scalabre, A.; Pouget, E.; Durola, F.; Coquerel, Y. Cyclobishelicenes: Shape-Persistent Figure-Eight Aromatic Molecules with Promising Chiroptical Properties. *Chem. Eur. J.* **2019**, *25*, 14364-14369.

(22) Fan, W.; Matsuno, T.; Han, Y.; Wang, X.; Zhou, Q.; Isobe, H.; Wu, J. Synthesis and Chiral Resolution of Twisted Carbon Nanobelts. *J. Am. Chem. Soc.* **2021**, *143*, 15924-15929.

(23) (a) Mitchell, R. H.; Boekelheide, V. Transformation of Sulfide Linkages to Carbon–Carbon Double Bonds. Synthesis of *cis*- and *trans*-15,16-Dimeyhyldihydropyrene and *trans*-15,16-Dihydropyrene. *J. Am. Chem. Soc.* **1974**, *96*, 1547-1557. (b) Bodwell, G. J.; Bridson, J. N.; Chen, S.-L.; Poirier, R. A. Nonplanar Aromatic Compounds. 5. A Strategy for the Synthesis of *cis*-10b,10c-Dimethyl-10b,10c-dihydropyrenes. First Crystal Structure of a *cis*-10b,10c-Dimethyl-10b,10c-dihydropyrene. *J. Am. Chem. Soc.* **2001**, *123*, 4704-4708. (c) Bodwell, G. J.; Miller, D. O.; Vermeij, R. J. Nonplanar Aromatic Compounds. 6. [2]Paracyclo[2](2,7)pyrenophane. A Novel Strained Cyclophane and a First Step on the Road to a "Vögtle" Belt. *Org. Lett.* **2001**, *3*, 2093-2096.

(24) (a) Yano, K.; Osatani, M.; Tani, K.; Adachi, T.; Yamamoto, K.; Matsubara, H. An Attempted Synthesis of 8-Shaped Circulene: Synthesis and Charaterization of [2.2](4,4')Biphenylo(3,11)dibenzo[*c,l*]chrysenophane and Its Cyclophadiene. *Bull. Chem. Soc. Jpn.* **2000**, *73*, 185-189. (b) Matsubara, H.; Yano, K.; Yamamoto, K. Syntheses and Characterizations of Dibenzochrysenophane and Biphenylodibenzochrysenophane Directed Toward Preparation of 8-shaped Closed Circulenes. *Polycl. Aromat. Comp.* **2001**, *19*, 165-177.

(25) Borch, R. F. Nitrilium Salts. New Method for the Synthesis of Secondary Amines. *J. Org. Chem.* **1969**, *34*, 627-629.

(26) Fuchter, M. J.; Weimar, M.; Yang, X.; Judge, D. K.; White, A. J. P. An unusual oxidative rearrangement of [7]-helicene. *Tetrahedron Lett.* **2012**, *53*, 1108-1111.

(27) Martin, R. H.; Marchant, M. J. Resolution and Optical Properties ([α]$_{max}$, ORD, and CD) of Hepta-, Octa- and Nonahelicene. *Tetrahedron* **1974**, *30*, 343-345.

(28) Birks, J. B.; Birch, D. J. S.; Cordemans, E.; Vander Donckt, E. Fluorescence of the Higher Helicenes. *Chem. Phys. Lett.* **1976**, *43*, 33-36.

(29) Vander Donckt, E.; Nasielski, J.; Greenleaf, J. R.; Birks, J. B. Fluorescence of the Helicenes. *Chem. Phys. Lett.* **1968**, *2*, 409-410.

(30) Frisch, M. J.; Trucks, G. W.; Schlegel, H. B.; Scuseria, G. E.; Robb, M. A.; Cheeseman, J. R.; Scalmani, G.; Barone, V.; Petersson, G. A.; Nakatsuji, H.; Li, X.; Caricato, M.; Marenich, A. V.; Bloino, J.; Janesko, B. G.; Gomperts, R.; Mennucci, B.; Hratchian, H. P.; Ortiz, J. V.; Izmaylov, A. F.; Sonnenberg, J. L.; Williams; Ding, F.; Lipparini, F.; Egidi, F.; Goings, J.; Peng, B.; Petrone, A.; Henderson, T.; Ranasinghe, D.; Zakrzewski, V. G.; Gao, J.; Rega, N.; Zheng, G.; Liang, W.; Hada, M.; Ehara, M.; Toyota, K.; Fukuda, R.; Hasegawa, J.; Ishida, M.; Nakajima, T.; Honda, Y.; Kitao, O.; Nakai, H.; Vreven, T.; Throssell, K.; Montgomery Jr., J. A.; Peralta, J. E.; Ogliaro, F.; Bearpark, M. J.; Heyd, J. J.; Brothers, E. N.; Kudin, K. N.; Staroverov, V. N.; Keith, T. A.; Kobayashi, R.; Normand, J.; Raghavachari, K.; Rendell, A. P.; Burant, J. C.; Iyengar, S. S.; Tomasi, J.; Cossi, M.; Millam, J. M.; Klene, M.; Adamo, C.; Cammi, R.; Ochterski, J. W.; Martin, R. L.; Morokuma, K.; Farkas, O.; Foresman, J. B.; Fox, D. J. *Gaussian 16 Rev. C.01*, Wallingford, CT, **2016**.

(31) Adamo, C.; Barone, V. Toward reliable density functional methods without adjustable parameters: The PBE0 model, *J. Chem. Phys.* **1999**, *110*, 6158-6169.

(32) (a) London, L. The quantic theory of inter-atomic currents in aromatic combinations, *J. Phys. Radium*, **1937**, *8*, 397-409. (b) McWeeny, R. Perturbation Theory for Fock-Dirac Density Matrix. *Phys. Rev.* **1962**, *126*, 1028. (c) Ditchfield, R. Self-consistent perturbation theory of diamagnetism. 1. Gauge-invariant LCAO method for N.M.R. chemical shifts. *Mol. Phys.* **1974**, *27*, 789-807. (d) Cheeseman, J. R.; Trucks, G. W.; Keith, T. A.; Frisch, M. J. A Comparison of Models for Calculating Nuclear Magnetic Resonance Shielding Tensors. *J. Chem. Phys.* **1996**, *104*, 5497-5509. (e) Ebrahimi, H. P.; Shaghaghi, H.; Tafazzoli, M. Gauge invariant atomic orbital-density functional theory prediction of accurate gas phase ^{1}H and ^{13}C NMR chemical shifts. *Concepts Magn. Reson.* **2011**, *38A*, 269-279.

(33) (a) Becke, A. D. Density-functional thermochemistry. III. The role of exact exchange. *J. Chem. Phys.* **1993**, *98*, 5648-5652. (b) Lee, C.; Yang, W.; Parr, R. G. Development of the Colle-Salvetti correlation-energy formula into a functional of the electron density. *Phys. Rev. B* **1988**, *37*, 785-789.

(34) Marenich, A. V.; Cramer, C. J.; Truhlar, D. J. Universal Solvation Model Based on Solute Electron Density and on a Continuum Model of the Solvent Defined by the Bulk Dielectric Constant and Atomic Surface Tensions. *J. Phys. Chem. B* **2009**, *113*, 6378-6396.

(35) (a) Schleyer, P. v. R.; Maerker, C.; Dransfeld, A.; Jiao, H.; van Eikema Hommes, N. J. R. Nucleus-Independent Chemical Shifts: A Simple and Efficient Aromaticity Probe. *J. Am. Chem. Soc.* **1996**, *118*, 6317-6318. (b) Chen, Z.; Wannere, C. S.; Corminboeuf, C.; Puchta, R.; Schleyer, P. V. R. Nucleus-Independent Chemical Shifts (NICS) as an Aromaticity Criterion. *Chem. Rev.* **2005**, *105*, 3842-3888.

(36) For reviews see: (a) Ito, H.; Ozaki, K.; Itami, K. Annulative π-Extension (APEX): Rapid Access to Fused Arenes, Heteroarenes, and Nanographenes. *Angew. Chem., Int. Ed.* **2017**, *56*, 11144-11164. (b) Ito, H.; Segawa, Y.; Murakami, K.; Itami K. Polycyclic Arene Synthesis by Annulative π-Extension. *J. Am. Chem. Soc.* **2019**, *141*, 3-10. For selected examples, see: (c) Ozaki, K.; Kawasumi, K.; Shibata, M.; Ito, H.; Itami, K. One-shot K-region-selective annulative π-extension for nanographene synthesis and functionalization. *Nat. Commun.* **2015**, *6*, 6251. (d) Matsuoka, W.; Ito, H.; Itami, K. Rapid Acceess to Nanographenes and Fused Heteroaromatics by Palladium-Catalyzed Annulative π-Extension Reaction of Unfunctionalized Aromatics with Diiodobiaryls. *Angew. Chem., Int. Ed.* **2017**, 56. 12224-12228. (e) Koga, Y.; Kaneda, T.; Saito, Y.; Murakami, K.; Itami, K. Synthesis of partially and fully fused polyaromatics by annulative chlorophenylene dimerization. *Science* **2018**, *359*, 435-439. (f) Kawahara, K. P.; Matsuoka, W.; Ito, H.; Itami, K. Synthesis of Nitrogen-Containing Polyaromatics by Aza-Annulative π-Extension of Unfunctionalized Aromatics. *Angew. Chem., Int. Ed.* **2020**, *59*, 6383-6388. (g) Matsuoka, W.; Ito, H.; Sarlah, D.; Itami, K. Diversity-oriented synthesis of nanographenes enabled by dearomative annulative π-extension. *Nat. Commun.* **2021**, *12*, 3940.

(37) (a) Mochida, K.; Kawasumi, K.; Segawa, Y.; Itami, K. Direct Arylation of Polycyclic Aromatic Hydrocarbons through Palladium Catalysis. *J. Am. Chem. Soc.* **2011**, *133*, 10716-10719. (b) Kawasumi, K.; Zhang, Q.; Segawa, Y.; Scott, L. T.; Itami, K. A grossly warped nanographene and the consequences of multiple odd-membered-ring defects. *Nat. Chem.* **2013**, *5*, 739-744. (c) Zhang, Q.; Kawasumi, K.; Segawa, Y.; Itami, K.; Scott, L. T. Palladium-Catalyzed C–H Activation Taken to the Limit. Flattening an Aromatic Bowl by Total Arylation. *J. Am. Chem. Soc.* **2012**, *134*, 15664-15667. (d) Shibata M.; Ito, H.; Itami, K. C–H Arylation of Phenanthrene with Trimethylphenylsilane by Pd/*o*-Chloranil Catalysis: Computational Studies on the Mechanism, Regioselectivity, and Role of *o*-Chloranil. *J. Am. Chem. Soc.* **2018**, *140*, 2196-2205. For reviews, see: (e) Segawa, Y.; Maekawa, T.; Itami, K. Synthesis of Extended π-Systems through C–H Activation. *Angew. Chem., Int. Ed.* **2015**, *54*, 66-81. (f) Stepek, I. A.; Itami, K. Recent Advances on C–H Activation for the Synthesis of π-Extended Materials. *ACS Mater. Lett.* **2020**, *2*, 951-974.

(38) Dennington, R.; Keith, T. A.; Millam, J. M. *GaussView, Version 6*, Semichem Inc., Shawnee Mission, KS, **2016**.

(39) Nakai, Y.; Mori, T.; Inoue, Y. Theoretical and Experimental Studies on Circular Dichroism of Carbo[*n*]helicenes. *J. Phys. Chem. A* **2012**, *116*, 7372-7385.

(40) Nakai, Y.; Mori, T.; Inoue, Y. Circular Dichroism of (Di)methyl- and Diaza[6]helicenes. A Combined Theoretical and Experimental Study. *J. Phys. Chem. A* **2013**, *117*, 83-93.

(41) Newman, M. S.; Lednicer, D. The Synthesis and Resolution of Hexahelicene. *J. Am. Chem. Soc.* **1956**, *78*, 4765-4770.

(42) Martin, R. H.; Marchant, M. J. Thermal racemisation of hepta-, octa-, and nonahelicene. *Tetrahedron* **1974**, *30*, 347-349.

(43) (a) Zhao, W.-L.; Li, M.; Lu, H.-Y.; Chen, C. F. Advances in helicene derivatives with circularly polarized luminescence. *Chem. Commun.* **2019**, *55*, 13793-13803. (b) Hasegawa, M.; Nojima, Y.; Mazaki, Y. Circularly Polarized Luminescence in Chiral π-Conjugated Macrocycles. *ChemPhotoChem*, Early View. DOI: 10.1002/cptc.202100162. (c) Tanaka, H.; Inoue, Y.; Mori, T. Circularly Polarized Luminescence and Circular Dichroisms in Small Organic Molecules: Correlation between Excitation and Emission Dissymmetry Factors. *ChemPhotoChem* **2018**, *2*, 386-402. (d) Nagata, Y.; Mori, T. Irreverent Nature of Dissymmetry Factor and Quantum Yield in Circularly Polarized Luminescence of Small Organic Molecules. *Front. Chem.* **2020**, *8*, 448. (e) Arrico, L.; Bari, D. D.; Zinna, F. Quantifying the Overall Efficiency of Circularly Polarized Emitters. *Chem. Eur. J.* **2021**, *27*, 2920-2934.

(44) (a) Morisaki, Y.; Gon, M.; Sasamori, T.; Tokitoh, N.; Chujo, Y. Planar Chiral Tetrasubstituted [2.2]Paracyclophane: Optical Resolution and Functionalization. *J. Am. Chem. Soc.* **2014**, *136*, 3350-3353. (b) Gon, M.; Morisaki, Y.; Chujo, Y. Optically active cyclic compounds based on planar chiral [2.2]paracyclophane: extension of the conjugated systems and chiroptical properties. *J. Mater. Chem. C* **2015**, *3*, 521-529. (c) Ushiyama, A.; Hiroto, S.; Yuasa, J.; Kawai, T.; Shinokubo, H. Synthesis of a figure-eight azahelicene dimer with high emission and CPL properties. *Org. Chem. Front.* **2017**, *4*, 664-667. (d) Saikawa, M.; Nakamura, T.; Uchida, J.; Yamamura, M.; Nabeshima, T. Synthesis of figure-of-eight helical bisBODIPY macrocycles and their chiroptical properties. *Chem. Commun.* **2016**, *52*, 10727-10730. (e) Robert, A.; Dechambenoit, P.; Hillard, E. A.; Durola, F. Non-planar oligoarylene macrocycles from biphenyl. *Chem. Commun.* **2017**, *53*, 11540-11543. (f) Senthilkumar, K.; Kondratowicz, M.; Lis, T.; Chmielewski, P. J.; Cybińska, J.; Zafra, J. L.; Casado, J.; Vives, T.; Crassous, J.; Favereau, L.; Stépień, M. Lemniscular [16]Cycloparaphenylene: A Radially Conjugated Figure-Eight Aromatic Molecule. *J. Am. Chem. Soc.* **2019**, *141*, 7421-7427. (g) Kubo, K.; Shimizu, D.; Hirose, T.; Matsuda, K. Circularly Polarized Luminescence Designed from Molecular Orbitals: A Figure-Eight-Shaped [5]Helicene Dimer with D_2 Symmetry. *Org. Lett.* **2020**, *22*, 9276-9281. (h) Xu, W.; Yang, X. D.; Fan, X. B.; Wang, X.; Tung, C. H.; Wu, L. Z.; Cong, H. Synthesis and Characterization of a Pentiptycene-Derived Dual Oligoparaphenylene Nanohoop. *Angew. Chem., Int. Ed.* **2019**, *58*, 3943-3947. (i) Nojima, Y.; Hasegawa, M.; Hara, N.; Imai, Y.; Mazaki, Y. Small Figure-Eight

Luminophores: Double-Twisted Tethered Cyclic Binaphthyls Boost
Circularly Polarized Luminescence. *Chem. Eur. J.* **2021**, *27*, 5923-5929.

Infinitene — A helically twisted figure-eight [12]circulene topoisomer ($C_{48}H_{24}$)